

Research Article

H₂O/O₂ Vapor Annealing Effect on Spin Coating Alumina Thin Films for Passivation of Silicon Solar Cells

Abdullah Uzum,¹ Hiroyuki Kanda,¹ Takuma Noguchi,¹ Yuya Nakazawa,¹ Shota Taniwaki,² Yasushi Hotta,² Yuichi Haruyama,¹ Naoyuki Shibayama,¹ and Seigo Ito ¹

¹Department of Materials and Synchrotron Radiation Engineering, University of Hyogo, 2167 Shosha, Himeji, Hyogo 671-2280, Japan

²Department of Electrical Engineering and Computer Sciences, University of Hyogo, 2167 Shosha, Himeji, Hyogo 671-2280, Japan

Correspondence should be addressed to Seigo Ito; itou@eng.u-hyogo.ac.jp

Received 3 January 2019; Accepted 25 February 2019; Published 17 March 2019

Guest Editor: Hui Wang

Copyright © 2019 Abdullah Uzum et al. This is an open access article distributed under the Creative Commons Attribution License, which permits unrestricted use, distribution, and reproduction in any medium, provided the original work is properly cited.

Aluminum acetylacetonate-based AlO_x thin films were introduced as a low-cost, high-quality passivation layers for crystalline silicon solar cells. Films were formed by a spin coating method on p-type silicon substrates at 450°C in ambient air, O₂, or water vapor (H₂O/O₂) for 15 or 120 min. XPS analysis confirms the AlO_x formation and reveals a high intensity of interfacial SiO_x at the AlO_x/Si interface of processed wafers. Ambient H₂O/O₂ was found to be more beneficial for the activation of introduced AlO_x passivation films which offers high lifetime improvements with a low thermal budget. Carrier lifetime measurements provides that symmetrically coated wafers reach 119.3 μs and 248.3 μs after annealing in ambient H₂O/O₂ for 15 min and 120 min, respectively.

1. Introduction

Reducing the production cost of Si solar cells is one of the major issues in photovoltaic industries, and many researchers have spent considerable efforts to reduce the material cost of silicon wafer which is a large part of the cost. Hence, the decreased use of silicon wafer (namely, the use of thin silicon wafers) provides a crucial solution for the cost-reduction problem. On the other hand, the solar cells of the thin silicon wafer have another serious problem in which the conversion efficiencies are decreased due to the carrier recombination dominantly at the surface region of the silicon wafer. Fortunately, surface passivation becomes one of the effective ways to solve the problem [1]. Furthermore, in order to achieve higher conversion efficiency (finally, to realize the theoretical efficiency limit) of front junction silicon solar cell, the back surface passivation is a key technology; the back surface field induced from the aluminum layer, which is formed by conventional screen printing, must be improved with alternative passivation layers with back surface fields and contact characteristics

[2–4]. Several passivation films such as a-Si:H, SiN_x, SiO₂, and AlO_x [5–8] have been studied in use for silicon solar cells. When applying SiO₂ and SiN_x to p⁺ emitters or local back surface fields, high-density positive charges cause strong parasitic shunting and lead to poor electrical characteristics of solar cell [9–11]. Therefore, passivation films with negative charges are needed for back surface passivation of high-efficiency p-type solar cells and for p⁺ emitter passivation in n-type solar cells. Surface passivation with AlO_x thin films with its excellent electrical properties is a suitable candidate as the passivation layer with negative charge effects. The widely used techniques to form high-quality AlO_x passivation films are atomic layer deposition (ALD) [2, 12, 13] and plasma-enhanced chemical vapor deposition (PECVD). However, apparatus costs are relatively expensive. Moreover, the use of hazardous precursors including trimethyl aluminum (TMA) in an ALD process [12] and resulting toxic byproducts when using the PECVD technique is the main drawback [14, 15]. On the other hand, AlO_x-based solutions [16, 17] which can be deposited by low-cost techniques including spin coating, spray pyrolysis, or screen

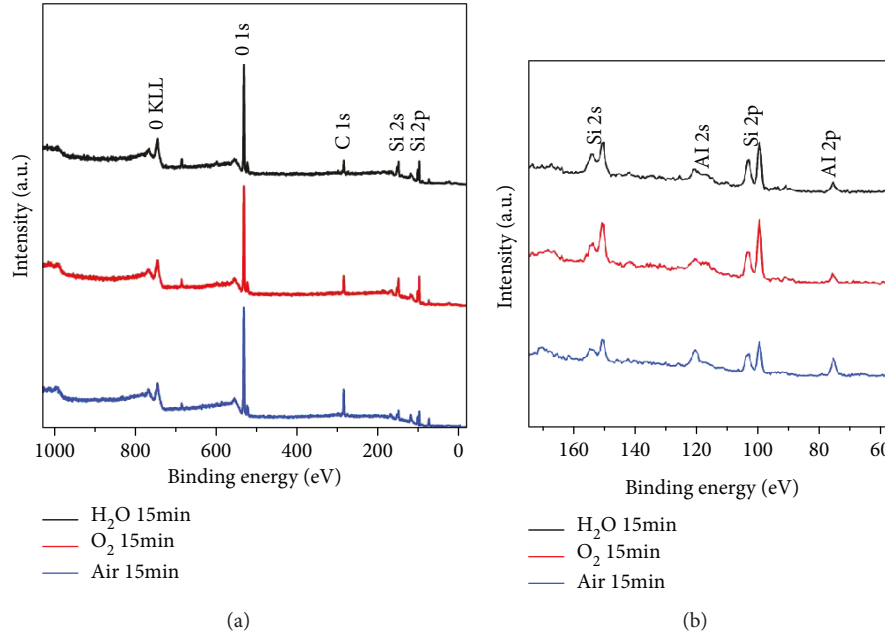


FIGURE 1: XPS spectra of Al-acac-based AlO_x formed in various ambients ($\text{H}_2\text{O}/\text{O}_2$, O_2 , and air): (a) wide spectrum (0-1000 eV) and (b) expansion spectrum (55-175 eV).

printing can be one of the alternatives to form low-cost, nontoxic AlO_x passivation layers for the use of solar cell applications. Investigations for the synthesis of such high-performance AlO_x layers and adaptation of them to the solar cell fabrication processes are crucial and still in demand.

In this work, spin coating aluminum oxide thin films based on aluminum acetylacetonate (Al-acac) were prepared and were investigated as a quality passivation layer material for p-type silicon substrates. Because the interface properties of the AlO_x film with the silicon substrate are crucial for high-quality passivation films, a special attention was given to the analysis of the interface, and the ambient effect during the activation process of the films was investigated which can significantly affect the resulting interface characteristics. Characterizations were carried out mainly by X-ray photoelectron spectroscopy (XPS) measurements and carrier lifetime studies by μ -PCD to determine the interface properties including the effective fixed charge density (Q_{eff}) changes before and after the applied processes.

2. Experimental

Aluminum acetylacetonate solution (Al-acac) was prepared by mixing of 0.486 g aluminum (III) acetylacetonate ($\text{Al}(\text{CH}_3\text{COCHCOCH}_3)_3$) (Wako Pure Chemical Ind. Ltd.) with 50 mL ethanol and stirred for 1 hour which provides a 0.03 M of Al-acac solution. 25 mm \times 25 mm-sized 10-50 Ω -cm p-type CZ-Si wafers (cut from 6-inch wafers) were used as a substrate. Prior to the Al-acac deposition, wafers were etched in acidic solution containing $\text{HF}:\text{HNO}_3$ (1:5 in volume) for 5 min and dipped into the 10% HF solution for 1 min to remove the native oxide at the surface of the substrate. Spin coating of Al-acac solution was performed

with the rotation speed of 4000 rpm, and coated samples were dried at 125°C for 5 min. A symmetrical structure was established by subsequent coatings on both sides of the wafers. The thickness of AlO_x thin films was \sim 2.8 nm measured by spectroscopic ellipsometry (model: Gonio bench, Sopra). Coated wafers were annealed in quartz furnace at 450°C in ambient air, O_2 , or water vapor ($\text{H}_2\text{O}/\text{O}_2$). The annealing time was varied between 15 and 120 min.

The initial effective lifetime estimation of cleaned silicon wafers was carried out using μ -PCD (WT-1000B, Semilab). Initial lifetimes of preprocessed wafers were around 10 μs . Similarly, postannealing effective carrier lifetimes of AlO_x -coated wafers were also measured by μ -PCD. The interfacial analysis of the AlO_x -coated wafers was carried out by X-ray photoelectron spectroscopy (XPS, XPS system at the synchrotron of beam line 7b, NewSUBARU, University of Hyogo). The energy offset was calibrated using the C 1s signal (284.8 eV). The cyclic voltammetry measurement was performed with an LCR instrument (E4980A, Agilent) to determine the Q_{eff} .

3. Results and Discussion

XPS measurements of Al-acac-based AlO_x films were carried out and were analyzed. The XPS survey spectrum of the Al-acac-based AlO_x films formed in various ambients ($\text{H}_2\text{O}/\text{O}_2$, O_2 , and air) in 15 min is given in Figure 1(a) with the highlighted peaks. Al 2s and Al 2p peaks can be confirmed for each processed ambient in an expanded spectrum in Figure 1(b).

Peaks corresponding to Al 2p were observed for all AlO_x layers formed in different ambients at a binding energy of \sim 76 eV [18]. Figure 2 shows detailed spectra of Al 2p core

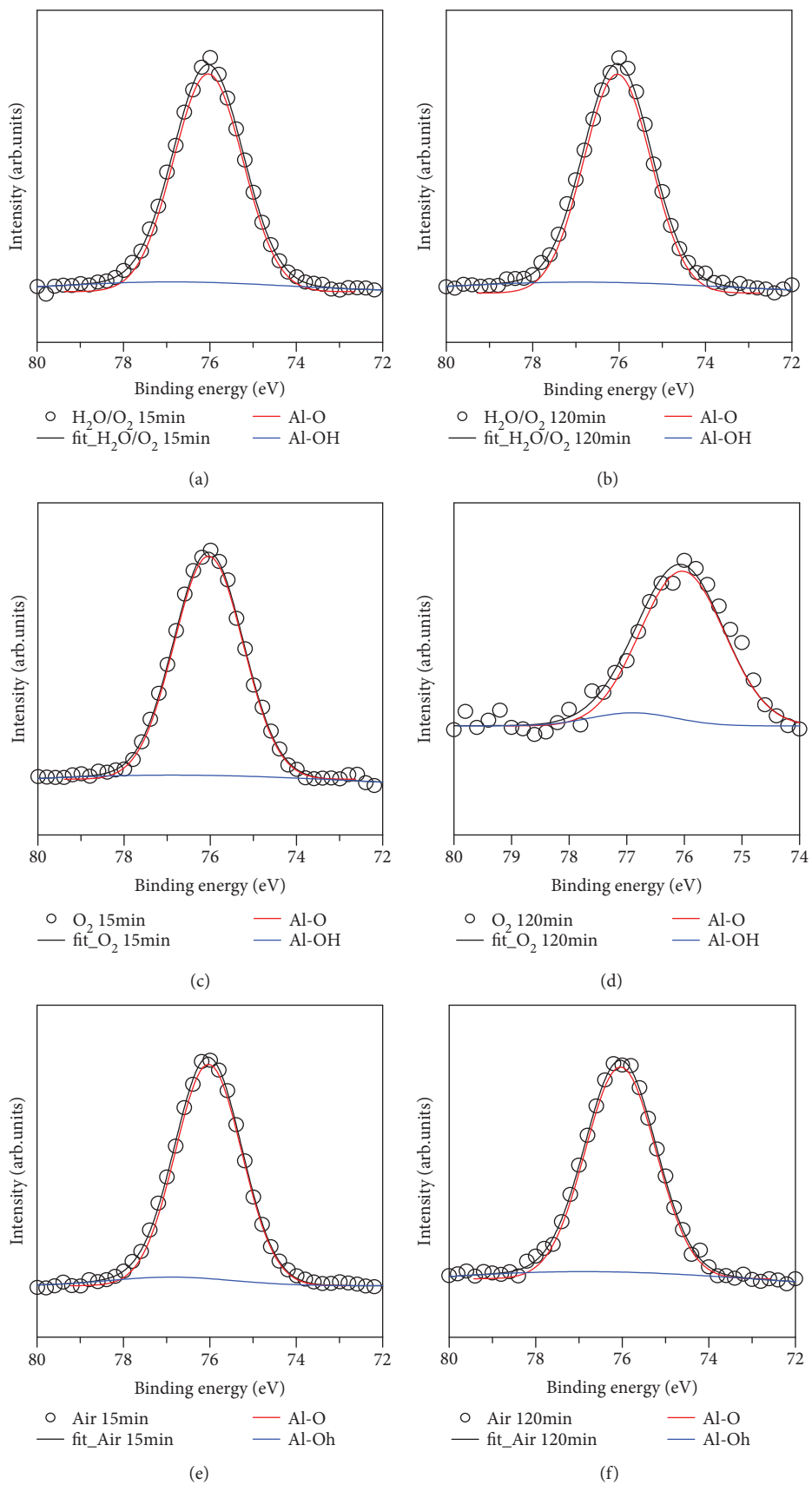


FIGURE 2: XPS Al 2p core level spectra of Al-acac-based AlO_x formed in ambient (a) $\text{H}_2\text{O}/\text{O}_2$ for 15 min, (b) $\text{H}_2\text{O}/\text{O}_2$ for 120 min, (c) O_2 for 15 min, (d) O_2 for 120 min, (e) air for 15 min, and (f) air for 120 min.

levels ((a, b) in $\text{H}_2\text{O}/\text{O}_2$; (c, d) in O_2 ; and (e, f) in air). Al 2p peaks were deconvoluted into the subpeaks representing Al-O and Al-OH bonds. The main contribution was from Al-O bonds, and the side signal was Al-OH bonds for all cases. Calculated area fractions of related subpeaks of Al-O and Al-OH are given in Table 1. Considering the areas of Al-O peaks for Al 2p core levels, these results show a clear elemental O and Al existence and confirm AlO_x films in nonstoichiometric ratios after processed conditions.

The peak of Si 2p was measured as well, by scanning around 98 to 106 eV by XPS measurement, and its decomposition was carried out in order to confirm interfacial SiO_x formation at the AlO_x/Si interface upon the activation of AlO_x films. According to the fitting of the peaks, the oxidation states of silicon can be observed in Figure 3, which is composed of chemical states of bulk silicon ($\text{Si } 2p_{3/2}$ and $\text{Si } 2p_{1/2}$) and of suboxide peaks including Si_2O , SiO , Si_2O_3 , and SiO_2 [19, 20].

Table 2 provides the calculated ratio of Si_2O , SiO , Si_2O_3 , and SiO_2 subpeaks and the resulting total SiO_x ($\text{Si}^{3+} - \text{O} + \text{Si}^{4+} - \text{O}$) ratio with respect to bulk silicon (assuming $(\text{Si } 2p_{3/2})\% + (\text{Si } 2p_{1/2})\% = 100\%$).

The ratio of SiO_x with respect to Si increased for all annealing conditions (ambient of $\text{H}_2\text{O}/\text{O}_2$, O_2 , or air) by increasing the annealing time. The highest ratios of SiO_x were observed after annealing in ambient $\text{H}_2\text{O}/\text{O}_2$ for both annealing times of 15 min and 120 min than those of values for ambient air or O_2 . The area ratios of interfacial SiO_x were 61.89% and 77.33% for annealing of 15 and 120 min, respectively, for the case of ambient $\text{H}_2\text{O}/\text{O}_2$.

Figure 4 compares the carrier lifetime dependence of AlO_x -coated wafers processed in ambient $\text{H}_2\text{O}/\text{O}_2$, in ambient O_2 , and in ambient air, for 15 or 120 min. Lifetimes of the wafers processed in ambient $\text{H}_2\text{O}/\text{O}_2$ were increased significantly than those of the wafers processed in ambient O_2 or in ambient air. Average lifetimes of 119.3 μs and 248.3 μs were achieved after annealing in ambient $\text{H}_2\text{O}/\text{O}_2$ for 15 and 120 min, respectively. In the case of annealing in ambient O_2 , an average lifetime of 40.1 μs was achieved after annealing for 15 min while a lifetime of 165.2 μs could be achieved after 120 min of annealing. Similarly, average lifetimes of 69.5 μs and 218 μs were achieved after annealing in ambient air for 15 and 120 min, respectively. It is noteworthy that ambient $\text{H}_2\text{O}/\text{O}_2$ provides better results in both 15 min and 120 min processing durations.

In carrier lifetime measurements by μ -PCD, free electron-hole pairs under the illuminated area are generated in the sample by an infrared semiconductor laser pulse. The concentration of the carriers and the conductivity of the sample change due to the generation and recombination of the excited carriers, where the decaying of the conductivity because of recombinations is measured by detecting the microwave reflectivity by a measure of time [21]. Since some carriers recombine in the bulk and some recombine near the surface, carrier lifetimes could be improved after AlO_x passivation owing to the reduction of surface recombination velocity or, in other words, the reduction of recombination rate of carriers on the surface of the wafers. Therefore,

TABLE 1: The ratio of each bonding peak for each annealing condition.

Time	Annealing condition	Al-O area (%)	Al-OH area (%)
15 min	$\text{H}_2\text{O}/\text{O}_2$	92.71	7.29
	O_2	91.95	8.05
	Air	95.50	4.50
120 min	$\text{H}_2\text{O}/\text{O}_2$	92.08	7.92
	O_2	93.25	6.75
	Air	88.44	11.56

lifetime improvements were mainly attributed to the effect of AlO_x passivation and can be explained by the elimination of the recombination centers including defects and dangling bonds at or near the surface owing to the formation of interfacial SiO_x [22, 23]. The increase of SiO_x at the interface increases the passivation quality and can reduce dangling bonds by bonding of the oxygen atoms of SiO_x with negatively charged Al atoms [24]. Therefore, higher average carrier lifetimes of silicon wafers annealed in ambient $\text{H}_2\text{O}/\text{O}_2$ after the deposition of AlO_x films by Al-acac solution can be related to the higher ratio of SiO_x at the Si/AlO_x interface.

In order to investigate further, capacitance-voltage (C-V) measurements (Agilent E4980A LCR meter) were conducted at 1 MHz. Metal/insulator/semiconductor structures of $\langle \text{Au}/\text{AlO}_x/\text{p-Si}/\text{Au} \rangle$ were prepared for C-V measurements with Al-acac-based AlO_x films as the insulator, shown in Figure 5(a). Au was deposited by a thermal evaporation method. The effective fixed charge density (Q_{eff}) were extracted from C-V measurements using the known methods for high-frequency measurements [25]. Figure 5(b) presents the comparison of resulting Q_{eff} for each processing condition. Considering these results, a possible explanation for the increase of carrier lifetimes after annealing for 120 min can be the dominant field effect over the change of trapped density when Q_{eff} is greater than 10^{12} cm^{-2} [26]. In the case of ambient O_2 , Q_{eff} , O_2 increases from $-2.05 \times 10^{12} \text{ cm}^{-2}$ (annealing for 15 min) to $-4.4 \times 10^{12} \text{ cm}^{-2}$ (annealing for 120 min).

These results show that carrier lifetimes and Q_{eff} increase by increasing the annealing duration. It is interesting to note that although the highest Q_{eff} values achieved when annealing were processed in ambient O_2 , the resulting carrier lifetimes were lower than those of the annealing processes held in ambient air or in ambient $\text{H}_2\text{O}/\text{O}_2$. These contradictory results may be due to the reaction of O_2 with the silicon surface that results in not only additional surface charge densities but also surface recombination centers. In the case of $\text{H}_2\text{O}/\text{O}_2$, on the other hand, owing to the emission of H atoms on the silicon surface, the minority carrier lifetimes can be higher despite of lower fixed charge densities.

Considering these results cumulatively, one can conclude that the quality passivation effect of spin coating AlO_x films could be obtained at the moderate annealing temperature of 450°C in relatively short annealing times (as low as 15 min) when using ambient $\text{H}_2\text{O}/\text{O}_2$. Therefore, spin

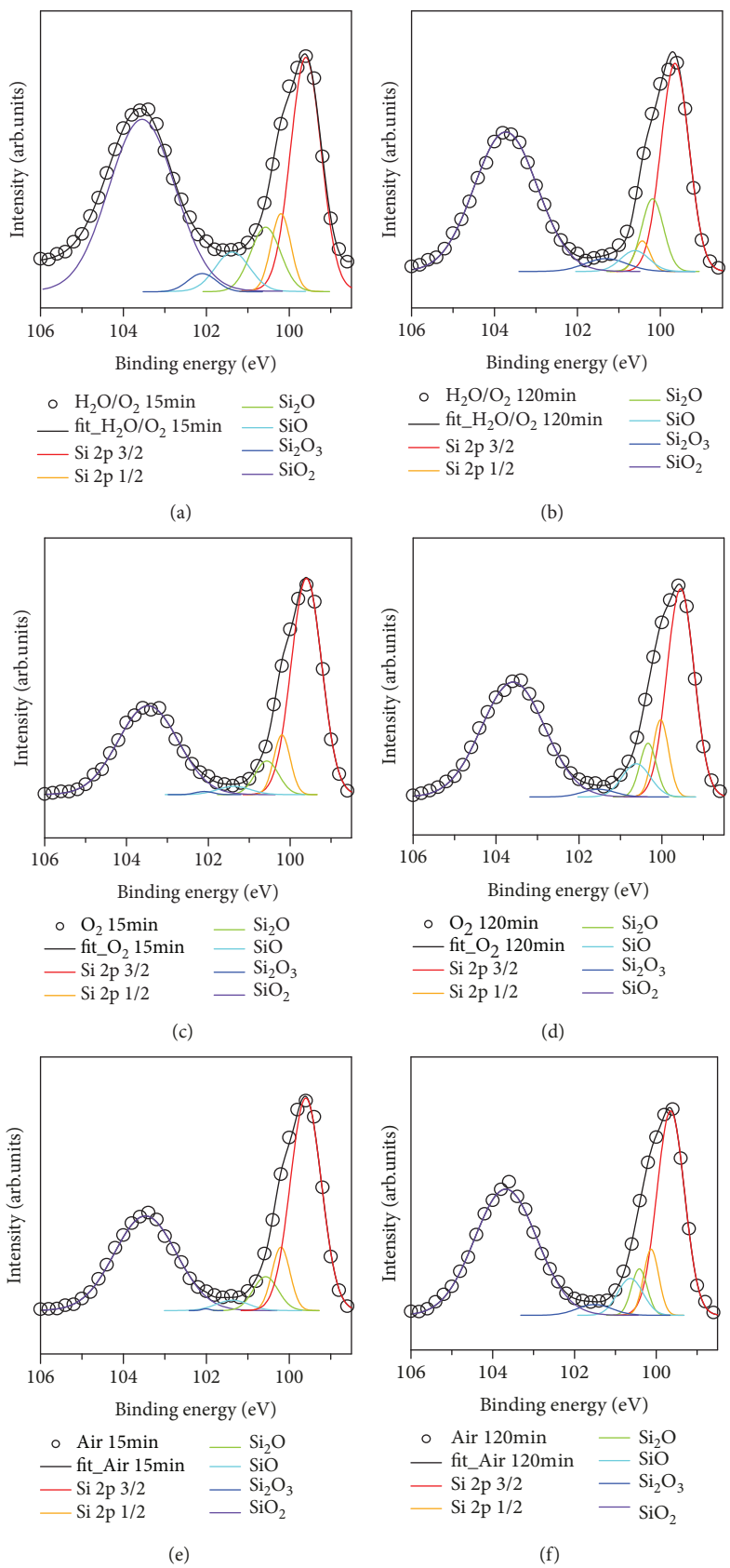


FIGURE 3: XPS Si 2p core level spectra with suboxides of Al-acac-based AlO_x films formed in ambient (a) $\text{H}_2\text{O}/\text{O}_2$ for 15 min, (b) $\text{H}_2\text{O}/\text{O}_2$ for 120 min, (c) O_2 for 15 min, (d) O_2 for 120 min, (e) air for 15 min, and (f) air for 120 min.

TABLE 2: The calculated ratio of silicon oxide subpeaks and total ratio of SiO_x after annealing of AlO_x film in various ambients for 15 or 120 min; criteria are based on Si peak.

Time	Annealing condition	Si^+-O (%)	$\text{Si}^{2+}-\text{O}$ (%)	$\text{Si}^{3+}-\text{O}$ (%)	$\text{Si}^{4+}-\text{O}$ (%)	SiO_x ($\text{Si}^{3+} + \text{Si}^{4+}$) (%)
15 min	$\text{H}_2\text{O}/\text{O}_2$	18.35	11.18	5.19	56.70	61.89
	O_2	10.69	2.63	1.00	31.15	32.15
	Air	10.78	3.28	0.55	33.52	34.07
120 min	$\text{H}_2\text{O}/\text{O}_2$	30.45	5.37	8.74	68.59	77.33
	O_2	18.82	11.64	2.69	46.14	48.83
	Air	17.18	13.67	3.97	54.28	58.25

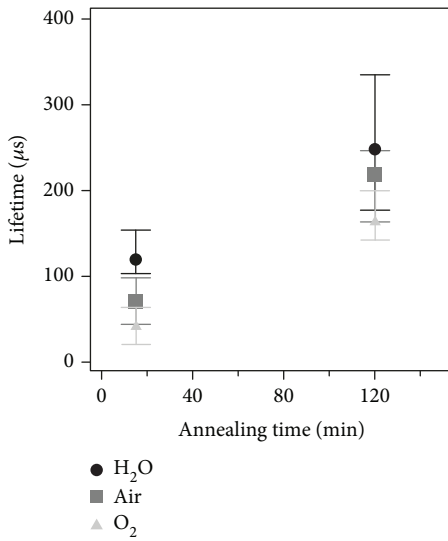


FIGURE 4: Effective carrier lifetime comparison of Al-acac-coated silicon wafers after annealing in different ambients ($\text{H}_2\text{O}/\text{O}_2$, O_2 , and air) for 15 or 120 min at 450°C .

coating Al-acac-based AlO_x films can be a promising low-cost and feasible alternative for the passivation of silicon substrates for crystalline silicon solar cell applications.

4. Conclusion

Cost-effective and simple process spin coatable aluminum acetylacetonate- (Al-acac-) based aluminum oxide films were introduced in this work. Carrier lifetime studies and XPS analysis were carried out for the evaluation of the films. The passivation performance of Al-acac-coated and subsequently annealed silicon substrates in ambient $\text{H}_2\text{O}/\text{O}_2$ was found to be more effective than that in ambient O_2 or ambient air. When annealing in ambient $\text{H}_2\text{O}/\text{O}_2$, the average lifetime reached around $119.3\ \mu\text{s}$ after processing only for 15 min which can lower the thermal budget of the cell fabrication process. Higher lifetimes of wafers annealed in ambient $\text{H}_2\text{O}/\text{O}_2$ were attributed to the greater SiO_x formation at the Si/ AlO_x interface and confirmed by XPS analysis. It can be concluded that Al-acac-based spin coating AlO_x films can be an attractive cost-effective candidate as a passivation layer for solar cell applications.

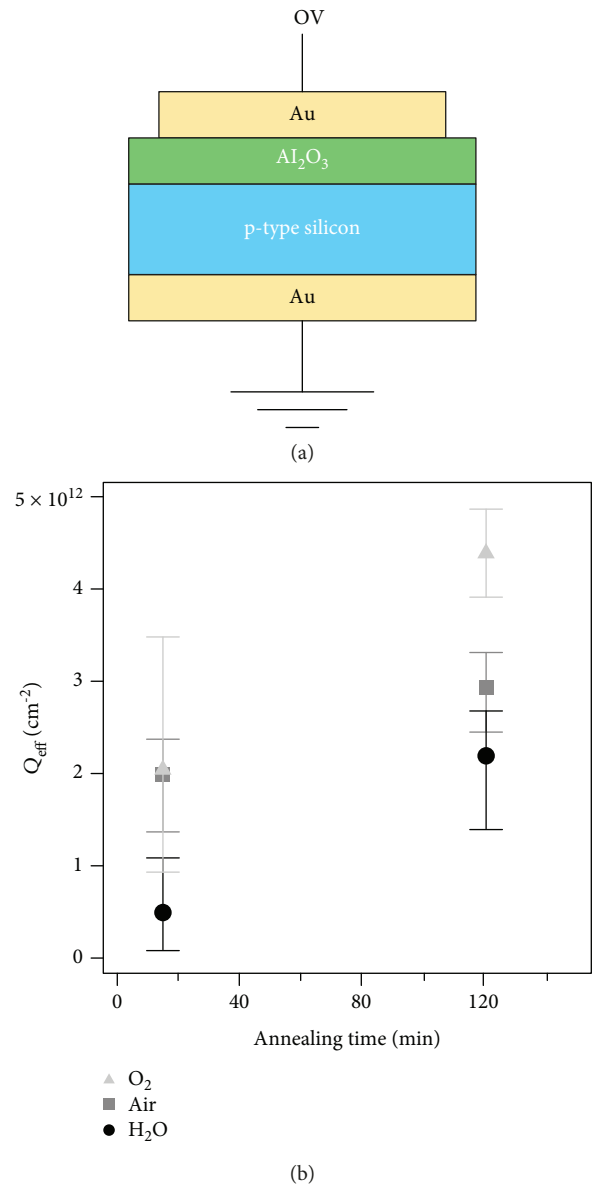


FIGURE 5: (a) Schematic of the device prepared for C-V measurement. (b) Effective charge density of the annealed sample in ambient $\text{H}_2\text{O}/\text{O}_2$, O_2 , and air for 15 or 120 min.

Data Availability

No data were used to support this study.

Disclosure

Abdullah Uzum's present address is at the Department of Electrical and Electronic Engineering, Karadeniz Technical University, Trabzon, 61080, Turkey.

Conflicts of Interest

The authors declare that they have no competing interests.

Acknowledgments

We are pleased to thank the staff of the NewSUBARU facility for their excellent support.

References

- [1] S. Bowden, F. Duerinckx, J. Szlufcik, and J. Nijs, "Rear passivation of thin multicrystalline silicon solar cells," *Opto-Electronics Review*, vol. 8, no. 4, pp. 307–310, 2000.
- [2] H. Huang, J. Lv, Y. Bao et al., "20.8% industrial PERC solar cell: ALD Al_2O_3 rear surface passivation, efficiency loss mechanisms analysis and roadmap to 24%," *Solar Energy Materials and Solar Cells*, vol. 161, pp. 14–30, 2017.
- [3] M. Müller, G. Fischer, B. Bitnar et al., "Loss analysis of 22% efficient industrial PERC solar cells," *Energy Procedia*, vol. 124, pp. 131–137, 2017.
- [4] M. A. Green, "The passivated emitter and rear cell (PERC): from conception to mass production," *Solar Energy Materials & Solar Cells*, vol. 143, pp. 190–197, 2015.
- [5] M. Agarwal, A. Pawar, N. Wadibhasme, and R. Dusane, "Controlling the c-Si/a-Si:H interface in silicon heterojunction solar cells fabricated by HWCVD," *Solar Energy*, vol. 144, pp. 417–423, 2017.
- [6] B. Zhang, Y. Zhang, R. Cong, Y. Li, W. Yu, and G. Fu, "Superior silicon surface passivation in HIT solar cells by optimizing a- SiO_x :H thin films: a compact intrinsic passivation layer," *Solar Energy*, vol. 155, pp. 670–678, 2017.
- [7] V. Titova, B. Veith-Wolf, D. Startsev, and J. Schmidt, "Effective passivation of crystalline silicon surfaces by ultrathin atomic-layer-deposited TiO_x layers," *Energy Procedia*, vol. 124, pp. 441–447, 2017.
- [8] L. E. Black, T. Allen, K. R. McIntosh, and A. Cuévas, "Improved silicon surface passivation of APCVD Al_2O_3 by rapid thermal annealing," *Energy Procedia*, vol. 92, pp. 317–325, 2016.
- [9] S. Dauwe, L. Mittelstadt, A. Metz, and R. Hezel, "Experimental evidence of parasitic shunting in silicon nitride rear surface passivated solar cells," *Progress in Photovoltaics: Research and Applications*, vol. 10, no. 4, pp. 271–278, 2002.
- [10] S. Gatz, T. Dullweber, V. Mertens, F. Einsele, and R. Brendel, "Firing stability of $\text{SiN}_x/\text{SiN}_x$ stacks for the surface passivation of crystalline silicon solar cells," *Solar Energy Materials & Solar Cells*, vol. 96, pp. 180–185, 2012.
- [11] I. Cesar, E. Bende, G. Galbiati, L. Janßen, A. Weeber, and J. H. Bultman, "All-side SiN_x passivated mc-Si solar cells evaluated with respect to parasitic shunting," in *2009 34th IEEE Photovoltaic Specialists Conference (PVSC)*, pp. 001386–001391, Philadelphia, PA, USA, June 2009.
- [12] F. Kersten, I. Förster, and S. Peters, "Evaluation of spatial ALD of Al_2O_3 for rear surface passivation of mc-Si PERC solar cells," in *Proceedings of 32nd European Photovoltaic Solar Energy Conference and Exhibition*, pp. 943–945, Munich, Germany, June 2016.
- [13] Y. Bao, H. Huang, Z. Zhu, J. Lv, and H. Savin, "Silicon surface passivation by mixed aluminum precursors in Al_2O_3 atomic layer deposition," *Energy Procedia*, vol. 92, pp. 304–308, 2016.
- [14] B. Kafle, S. Kuehnhold, W. Beyer et al., "Thermal stability investigations of PECVD Al_2O_3 films discussing a possibility of improving surface passivation by re-hydrogenation after high temperature processes," in *Proceedings of 27th European photovoltaic solar energy conference*, pp. 1788–1792, Frankfurt, Germany, September 2012.
- [15] M. Hofmann, N. Kohn, F. Schwarz et al., "High-power-plasma PECVD of SiN_x and Al_2O_3 for industrial solar cell manufacturing," in *Proceedings of 28th European Photovoltaic Solar Energy Conference and Exhibition*, pp. 1184–1187, Paris, France, September–October 2013.
- [16] N. Balaji, C. Park, J. Raja et al., "Low surface recombination velocity on p-type CZ-si surface by sol-gel deposition of Al_2O_3 films for solar cell applications," *Journal of Nanoscience and Nanotechnology*, vol. 15, no. 7, pp. 5123–5128, 2015.
- [17] M. Szindler, L. A. Dobrzański, M. M. Szindler, M. Pawlyta, and T. Jung, "Comparison of surface morphology and structure of Al_2O_3 thin films deposited by sol-gel and ALD methods," *Journal of Achievements in Materials and Manufacturing Engineering*, vol. 2, no. 82, pp. 49–57, 2017.
- [18] J. Haeberle, K. Henkel, H. Gargouri et al., "Ellipsometry and XPS comparative studies of thermal and plasma enhanced atomic layer deposited Al_2O_3 -films," *Beilstein Journal of Nanotechnology*, vol. 4, pp. 732–742, 2013.
- [19] R. Alfonsetti, L. Lozzi, M. Passacantando, P. Picozzi, and S. Santucci, "XPS studies on SiO_x thin films," *Applied Surface Science*, vol. 70-71, Part 1, pp. 222–225, 1993.
- [20] R. Alfonsetti, G. De Simone, L. Lozzi, M. Passacantando, P. Picozzi, and S. Santucci, " SiO_x surface stoichiometry by XPS: a comparison of various methods," *Surface and Interface Analysis*, vol. 22, no. 1-12, pp. 89–92, 1994.
- [21] *WT-1000B User Manual*, SEMILAB Inc., Budapest, Hungary, 2008.
- [22] B. Hoex, S. B. S. Heil, E. Langereis, M. C. M. van de Sanden, and W. M. M. Kessels, "Ultralow surface recombination of c-Si substrates passivated by plasma-assisted atomic layer deposited Al_2O_3 ," *Applied Physics Letters*, vol. 89, no. 4, article 042112, 2006.
- [23] S.-Y. Lien, C.-H. Yang, K.-C. Wu, and C.-Y. Kung, "Investigation on the passivated Si/ Al_2O_3 interface fabricated by non-vacuum spatial atomic layer deposition system," *Nanoscale Research Letters*, vol. 10, no. 1, p. 93, 2015.
- [24] A. M. Albadri, "Characterization of Al_2O_3 surface passivation of silicon solar cells," *Thin Solid Films*, vol. 562, pp. 451–455, 2014.
- [25] S. M. Sze, *Physics of Semiconductor Devices*, Bell Laboratories, Incorporated A Wiley Interscience publication, John Wiley and Sons, Murray Hill, New Jersey, USA, Second edition, 1981.
- [26] S. Miyajima, "Surface passivation films for crystalline silicon solar cells," *Journal of Plasma and Fusion Research*, vol. 85, p. 820, 2009.



Hindawi

Submit your manuscripts at
www.hindawi.com

